Applied GIS

ISSN: 1832-5505

Vol-09 Issue-03 July 2021

Droop-Controlled DC Microgrids: Mesh and Radial Configurations for Improved Load Power Sharing

G VENGALARAO[1] , MUSALI SUREKHA[2]

Associate professor[1,2]

DEPARTMENT OF ELECTRICAL AND ELECTRONICS ENGINEERING

P.B.R.VISVODAYA INSTITUTE OF TECHNOLOGY & SCIENCE

S.P.S.R NELLORE DIST, A.P , INDIA , KAVALI-524201

Abstract:

The capacity of the converters at each interface should be used to allocate electricity equitably. This work proposes a revised technique for improving the accuracy of load power sharing in droop-controlled DC microgrids, with the goal of ensuring that each converter performs under optimal conditions while taking into account the radial and mesh configurations. By using both average output power control and average DC voltage management of surrounding converters, two compensating terms are used. The communication network may be simplified by using just the nearby converter's data. Modified droop control, which may be thought of as a distributed method, is used to achieve the reasonable distribution of load power under varying line resistance circumstances. Sampled data is sent across converters via low bandwidth communication. Different network topologies and line resistances under varying communication delays are investigated in depth to determine the feasibility and efficacy of the proposed strategy. The suggested method is validated by simulation results obtained from a MATLAB/Simulink implementation of a DC microgrid with three converters. A 3x10kW prototype's experimental findings demonstrate the efficacy of the suggested updated droop control technique as well.

Keywords:

Communication lag, droop management, load power sharing, mesh and radial layouts, direct current microgrids

Introduction

Creating and using renewable energy sources is a major topic of discussion today [1,2]. Microgrids are gaining popularity as a means of coordinating the management of several forms of renewable energy [3]. Most microgrids use alternating current (AC) distribution like typical grids. However, the photovoltaic (PV) system, the fuel cell, and energy storage devices all provide DC output. As a result, DC-type microgrids may be more useful in boosting efficiency and enhancing power quality. Transmission lines are used to convey electricity generated at various locations to consumers, making it crucial that the electricity be transmitted efficiently and distributed fairly [4, 5]. At the same time, power electronic converters are crucial in DG owing to the mandates of renewable energy laws. An enhanced droop control approach was introduced in [10] to cut down on line loss and boost DC power system efficiency generally by preventing circulating currents among converters without utilizing specialized communication between them [6]. Both the voltage drop and the precision of load distribution may be improved with this technique employed at the same time. Since sampling data from all converters is required, there is an additional downside of high communication traffic. At the same time, we focus only on radial arrangement. This work proposes a refined version of the droop control strategy to

address these issues. The average voltage and output power of the neighboring converters are chosen as the regulating factors. Using just the information from neighboring converters keeps the communication load low. Each converter's voltage and power data is sent through a network with a relatively small data transmission rate. This technique discusses the impact of line impedance and the precision of power sharing. The lack of a central controller in the control system also has the potential to increase the method's stability. Research is conducted on both the mesh and radial system designs. Case studies based on both system configurations, generated via simulation and experimental data, show that the suggested strategy is both practical and effective. This section serves as the paper's outline. The problems with conventional droop management are addressed in Section 2. Section 3 then analyzes problems with droop control. Section 4 covers the topic of enhanced droop regulation. Section 5 then contrasts the simulated findings with the experimental results.

Conventional Methods of Sagging Control Current Developments in Direct Current Microgrids

DC microgrids have been the subject of much research in recent years because to the rising prevalence of distributed sources with DC output such photovoltaic (PV), battery storage, and the fuel cell. The following examples highlight their benefits, which extend to technical areas of control as well as cost-effective operation and efficiency:

ISSN: 1832-5505
Vol-09 Issue-03 July 2021

DC microgrids have easier modelling and control since there is no phase angle, frequency, or reactive power; AC systems have more complex control systems because of the need to account for synchronization, reactive power flow, and harmonics. Moreover, DC is favored over AC because it is compatible with the vast majority of today's electronic loads, energy storage devices, and DG technologies. The total cost of ownership, infrastructure, equipment, maintenance, and operation are all lower in DC microgrids, and the existing literature highlights this fact. • Economical operation [13-15]: Economical operation in DC microgrids can be achieved without complex and computation-intensive optimization algorithms. Effectiveness (16-18): As inverter conversion losses between DC output sources and loads are decreased, overall system efficiency improves. Due to the DC capacitor's stored energy and the AC/DC converter's voltage management, DC microgrids have an inherent fault-ride-through capacity.

Consideration of Controlling Drooping

The following analysis examines the aforementioned problems with the conventional droop control approach, paying special attention to the mesh and radial layouts.

Mesh Layout

The converter output current for mesh and radial configurations in DC microgrids may be computed by utilizing the stated voltage and current equations based on the numerous nodes of the simplified system models. The Kirchhoff's law-derived circuit equations are shown in Figure 2a below.

$$\begin{cases} v_L = R_L \cdot i_L \\ i_L = i_{dc1} + \dfrac{v_{dc2} - v_{dc1}}{r_{1L}} + i_{dc3} + \dfrac{v_{dc2} - v_{dc3}}{r_{3L}} \end{cases}$$

$$\begin{cases} i_{dc1} = \dfrac{v_{dc1} - v_L}{r_{1L}} - \dfrac{v_{dc2} - v_{dc1}}{r_{12}} \\ i_{dc2} = \dfrac{v_{dc2} - v_{dc1}}{r_{12}} + \dfrac{v_{dc2} - v_{dc3}}{r_{23}} \\ i_{dc3} = \dfrac{v_{dc3} - v_L}{r_{3L}} - \dfrac{v_{dc2} - v_{dc3}}{r_{23}} \end{cases}$$

where vdci is DC side output voltage of converter # i (i = 1, 2, 3), idci is DC side output current, vL is load voltage, iL is load side current, RL is load side resistance, rij (i = 1, 2, 3, j = 2, 3) is line resistance between different converters; Ri is the virtual resistance. Based on above circuit analysis and combining Equations (2) and (3), DC side output current can be obtained:

$$\begin{cases} i_{dc1} = \dfrac{1}{\lambda}\begin{pmatrix} [-(R_3 + 2R_L + r_{1L})r_{23}^2 - (R_2R_3 + 2R_2R_L + 2R_3R_L - R_2r_{3L} - R_3r_{3L})r_{23} - 2R_2R_3R_L]r_{12}^2 v_{dc}^* \\ -[R_2r_{23}^2(R_3 + r_{1L}) + 2R_2R_L r_{23}(R_3 + r_{23}) + R_2R_3r_{23}(r_{3L} + r_{1L})]r_{12}v_{dc}^* \end{pmatrix} \\ i_{dc2} = \dfrac{1}{\lambda}\begin{pmatrix} (-R_1R_3r_{23} - 2R_3R_Lr_{23} - R_3r_{23}r_{1L})r_{12}^2 v_{dc}^* \\ -[R_1R_3r_{23}(r_{23} + r_{3L} + r_{1L}) + R_3r_{23}^2(2R_L + r_{1L}) + 4R_1R_3R_Lr_{23}]r_{12}v_{dc}^* \end{pmatrix} \\ i_{dc3} = \dfrac{1}{\lambda}\begin{pmatrix} [-(R_1 + r_{1L})r_{23}^2 - (R_1R_2 + 2R_2R_L + R_2r_{1L})r_{23}]r_{12}^2 v_{dc}^* \\ -[(2R_L + r_{3L})(R_1 + R_2)r_{23}^2 + R_1R_2r_{23}(r_{3L} + r_{23} + r_{1L} + 2R_L)]r_{12}v_{dc}^* - 2R_1R_2R_Lr_{23}^2 v_{dc}^* \end{pmatrix} \end{cases}$$

Where

$$\lambda = \begin{pmatrix} 2R_2R_3R_L^2 - (r_{1L}r_{3L} + R_1R_3 + R_1R_L + R_2r_{3L} + R_3R_L + R_3r_{1L} + R_Lr_{1L} + R_Lr_{3L})r_{23}^2 - \\ [(r_{3L}r_{1L} + 2R_Lr_{3L})(R_2 + R_3) + (R_1 + R_L)R_1R_2 + (R_1 + R_2)R_3R_L + (R_2R_3 + R_2R_L + R_3R_L)r_{1L}]r_{23} \end{pmatrix} r_{12}^2$$
$$- \begin{pmatrix} [(R_3 + R_L)R_1R_2 + (R_1 + R_2)(R_3R_L + R_3r_{1L} + R_Lr_{1L} + R_Lr_{3L} + r_{1L}r_{3L}) + R_1R_2r_{3L}]r_{23}^2 - \\ [2R_2R_L^2(R_3 + R_1) - [(R_1 + R_2)R_3R_L + (R_1 + R_L)R_1R_2](r_{1L} + r_{3L}) - R_3r_{1L}r_{3L}(R_2 + R_3) - R_2R_3r_{1L}r_{3L}]r_{23} \\ -2R_1R_2R_3R_L(2R_L + r_{1L}) \end{pmatrix} r_{12}$$
$$+ 2R_1R_2R_Lr_{23}(R_1r_{23} + 2R_1R_L + R_1r_{3L})$$

In DC microgrids, by using traditional droop control method, accurate load power sharing accuracy can be obtained when the converter DC output power is set to be inversely proportional to the corresponding droop coefficient, the following expression can be obtained:

$$\frac{m_0}{k_1}\underbrace{[i_{dc1}(v_{dc}^* - \frac{m_0}{k_1}i_{dc1}v_{dc1})]}_{P_{dc1}} = \frac{m_0}{k_2}\underbrace{[i_{dc2}(v_{dc}^* - \frac{m_0}{k_2}i_{dc2}v_{dc2})]}_{P_{dc2}} = \frac{m_0}{k_3}\underbrace{[i_{dc3}(v_{dc}^* - \frac{m_0}{k_3}i_{dc3}v_{dc3})]}_{P_{dc3}}$$

Based on the above analysis, it can be seen that the power sharing error can be eliminated if and only if the droop coefficient and line impedance satisfy the relationship in Equation (5). However, this assumption is only suitable for an ideal system and the practical system is not satisfied. This is the limitation of the traditional droop control method in the mesh configuration of DC microgrids.

Proposed Approach In order to solve

the two problems of induced traditional droop control, this paper proposes a method of controlling the average values of the DC-link voltage of adjacent converters as well as the output power to compensate the voltage deviation induced by droop control, and simultaneously improve the load power sharing accuracy. The whole control diagram of the system is given in Figure 4. Compared to the existing method of averaging the voltage and power based on global information, the improved control method alleviates the communication traffic and further reduces the dependence on the communication system. The

ISSN: 1832-5505
Vol-09 Issue-03 July 2021

DC-link voltage references of the two adjacent converters are as follows:

$$v_{dci}^{*} = v_{dc}^{*} - \frac{m_0}{k_i} P_{dc} \cdot G_{LPF} + \underbrace{\left(v_{dc}^{*} - \frac{G_d \cdot v_{dc(i-1)} + G_d \cdot v_{dc(i+1)}}{2}\right) \cdot G_{piv}}_{\text{Compensating Controller I}} - \underbrace{\left(P_{dc}/k_i - \frac{G_d \cdot P_{dc(i-1)} + G_d \cdot P_{dc(i+1)}}{2}\right) \cdot G_{pip}}_{\text{Compensating Controller II}}$$

where ݒ݀ܿ□ ∗ is output DC-link voltage reference of the ith converter, ݒ݀ܿ∗ is line DC-link voltage reference,

$$v_{dc(i-1)} \text{ and } v_{dc(i+1)}$$

are the output voltages of the ith converter's two adjacent converters, ܲ݀ܿ□ is the ith converter's output power?ܿ

$$P_{dc(i-1)} \text{and } P_{dc(i+1)}$$

are the output power of the itch converter's two adjacent converters, ki is the proportional sharing accuracy of output power, m0 is the coefficient of traditional droop control, GLPF is low pass filter introduced in droop control, ωs is the cut-off frequency of the filter, Gpiv and Gpip are two compensating terms of improved droop control: The averaging voltage controller and averaging power controller, are both traditional PI controllers. The communication delay of the transfer variable is Gd, which can be expressed as the following

$$G_{pip} = k_{pp} + \frac{k_{ip}}{s}$$

$$G_{piv} = k_{pv} + \frac{k_{iv}}{s}$$

$$G_d = \frac{1}{1 + \tau s}$$

in the control system, low bandwidth communication is employed to transfer the sampling data of the DC-link voltage and power values between different converter units. Voltage deviations induced by droop control can be eliminated by PI controllers I for the average values of DC-link voltage and power respectively. However, there is a variety of renewable energy distributed into microgrids by multiple converters, which are separate and have no need of high frequency telecommunication lines. Hence, the sampling for all the transmission voltage and power between the converters will cause unnecessary errors

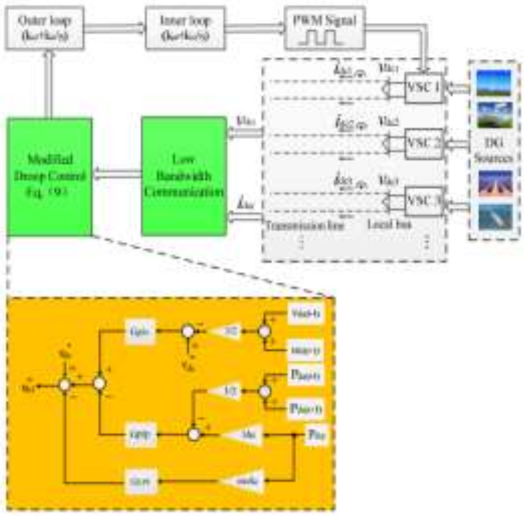

Figure 4. Detailed diagram of the proposed droop control system.

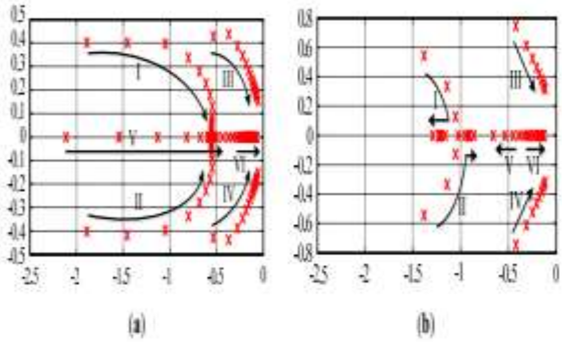

Figure 5. Closed-loop dominant poles for varying communication delay. (a) Mesh configuration (b) Radial configuration.

When communication delays are changed from 1 second to 10 seconds, as shown in Figure 5b, the position of the dominating closed-loop poles in the radial design shifts. The stability of the system is not compromised since poles I, II, and V remain on the left side of the s plane. However, if communication latency and loss increase, poles III, IV, and VI shift toward an imaginary axis, leading to an unstable state.

Compilations with Real-World Data

The performance of the suggested approach of better droop control was simulated using MATLAB/Simulink, and the viability of the control method was confirmed by taking into account varied line resistance rij, and communication latency, based on two distinct configurations. Table 1 displays the DC microgrids system's parameters. When comparing converters, the DC side power and DC side voltage are defined as follows, with maximum and lowest values shown in parentheses.

ISSN: 1832-5505
Vol-09 Issue-03 July 2021

$$\varepsilon_j = \max(P_{dci}) - \min(P_{dci})$$

$$\varepsilon_j \leq 0.1 \times P_{dci}$$

$$\delta_j = \max(v_{dci}) - \min(v_{dci})$$

$$\delta_j \leq 0.05 \times v_{dci}$$

where i = 1, 2, 3 denotes the converter's sequence number, j = 1, 2, 3, 4 denotes the type of specific case.

Table 1. DC microgrids system parameters

Item	Symbol	Value
Reference of DC output voltage	v_{dc}	380 V
Load resistance	R_L	19 Ω
Power sharing proportion (Converter #i=1,2,3)	k_i	1
LPF cutting frequency	f_c	20 Hz
Communication delay	τ	0.1 s or 1 s
Droop coefficient	m_0	0.0015
Averaging voltage controller proportion coefficient	k_{pv}	2×10^{-1}
Averaging voltage controller integral coefficient	k_{iv}	4.5×10^{-2}
Averaging power controller proportion coefficient	k_{pp}	2.3×10^{-3}
Averaging power controller integral coefficient	k_{ip}	5.5×10^{3}

Mesh configuration						Radial configuration				
Case No.	r_{1L}	r_{12}	r_{23}	r_{3L}	τ	Case No.	r_{1L}	r_{2L}	r_{3L}	τ
1	0.8 Ω	1.0 Ω	1.0 Ω	1.2 Ω	0.1 s	4	0.8 Ω	1.0 Ω	1.2 Ω	0.1 s
2	0.8 Ω	1.0 Ω	1.0 Ω	1.2 Ω	1 s	5	0.8 Ω	1.0 Ω	1.2 Ω	1 s
3	0.6 Ω	1.2 Ω	1.2 Ω	1.8 Ω	1 s	6	0.6 Ω	1.2 Ω	1.8 Ω	1 s

Conclusions

A modified distributed control approach for mesh and radial layout was presented and investigated to enhance the overall performance of a droop-controlled DC microgrid. This paper's main arguments are summed up as follows: (1) Both mesh and radial topologies were shown to be capable of ensuring the feasibility and stability of the control system. (2) The updated droop control approach may reduce local DC output voltage variation and improve the accuracy of load power sharing. Third, the suggested control approach only uses voltage and current data sampled from two neighbouring converters, making the communication system less taxed. (4) The control system is reliable, even with a bigger mismatch in line resistance and a longer communication delay time.

References

[1]. Dasgupta, S.; Mohan, S.N.; Sahoo, S.K.; Panda, S.K. Application of four-switch-based three-phase grid-connected inverter to connect renewable energy source to a generalized unbalanced microgrid system. IEEE Trans. Ind. Electron. 2013, 60, 1204–1215.

[2]. Hakimi, S.M.; Moghaddas-Tafreshi, S.M. Optimal planning of a smart microgrid including demand response and intermittent renewable energy resources. IEEE Trans. Smart Grid 2014, 5, 2889–2900.

[3]. Eghtedarpour, N.; Farjah, E. Distributed charge/discharge control of energy storages in a renewable-energy-based DC micro-grid. IET Renew. Power Gener. 2014, 8, 45–57.

[4]. Vandoorn, T.L.; de Kooning, J.D.M.; Meersman, B.; Guerrero, J.M.; Vandevelde, L. Automatic power-sharing modification of P/V droop controllers in low-voltage resistive microgrids. IEEE Trans. Power Deliv. 2012, 27, 2318–2325.

[5]. Augustine, S.; Mishra, M.; Lakshminarasamma, N. Adaptive droop control strategy for load sharing and circulating current minimization in low-voltage standalone DC microgrid. IEEE Trans. Sustain. Energy 2015, 6, 132–141.

[6]. Guerrero, J.M.; Vasquez, J.C.; Matas, J.; de Vicuña, L.G.; Castilla, M. Hierarchical control of droop-controlled AC and DC microgrids—A general approach toward standardization. IEEE Trans. Ind. Electron. 2011, 58, 158–172.

[7]. Rouzbehi, K.; Miranian, A.; Candela, J.I.; Luna, A.; Rodriguez, P. A generalized voltage droop strategy for control of multiterminal DC grids. IEEE Trans. Ind. Appl. 2015, 51, 607–618.

[8]. Bevrani, H.; Shokoohi, S. An intelligent droop control for simultaneous voltage and frequency regulation in islanded microgrids. IEEE Trans. Smart Grid 2013, 4, 1505–1513.

[9]. Dou, X.; Quan, X.; Wu, Z. Improved control strategy for microgrid ultracapacitor energy storage systems. Energies 2014, 7, 8095–8115.

[10]. Lu, X.; Guerrero, J.M.; Sun, K.; Vasquez, J.C. An improved droop control method for DC microgrids based on low bandwidth communication with DC bus voltage restoration and enhanced current sharing accuracy. IEEE Trans. Power Electron. 2014, 29, 1800–1812.

[11]. Maknouninejad, A.; Qu, Z.; Lewis, F.L.; Davoudi, A. Optimal, nonlinear, and distributed designs of droop controls for dc microgrids. IEEE Trans. Smart Grid 2014, 5, 2508–2516.

[12]. Wang, B.; Sechilariu, M.; Locment, F. Intelligent DC microgrid with smart grid communications: Control strategy consideration and design. IEEE Trans. Smart Grid 2012, 3, 2148–2156.

[13]. Liang, C.; Shahidehpour, M. DC Microgrids: Economic operation and enhancement of resilience by hierarchical control. IEEE Trans. Smart Grid 2014, 5, 2517–2526.

[14]. Kanchev, H.; Colas, F.; Lazarov, V.; Francois, B. Emission reduction and economical optimization of an urban microgrid operation including dispatched pv-based active generators. IEEE Trans. Sustain. Energy 2014, 5, 1397–1405.

[15]. Nutkani, I.U.; Wang, P.; Poh, C.L.; Blaabjerg, F. Autonomous economic operation of grid connected DC microgrid. In Proceedings of the 2014 IEEE 5th International

Symposium on Power Electronics for Distributed Generation Systems (PEDG), Galway, Ireland, 24–27 June 2014; pp. 1–5.

[16]. Kwasinski, A. Quantitative evaluation of DC microgrids availability: Effects of system architecture and converter topology design choices. IEEE Trans. Power Electron. 2011, 26, 835–851.

17]. Yukita, K.; Shimizu, Y.; Goto, Y.; Yoda, M.; Ueda, A.; Ichiyanagi, K.; Hirose, K.; Takeda, T.; Ota, T.; Okui, Y.; et al. Study of AC/DC power supply system with DGs using parallel processing method. In Proceedings of the International Power Electronics Conference (IPEC)-ECCE, Sapporo, Japan, 21–24 June 2010; pp. 722–725.

[18]. Kakigano, H.; Miura, Y.; Ise, T. Low-voltage bipolar-type DC microgrid for super high quality distribution. IEEE Trans. Power Electron 2010, 25, 3066–3075.

[19]. Shadmand, M.B.; Balog, R.S. Multi-objective optimization and design of photovoltaic-wind hybrid system for community smart DC microgrid. IEEE Trans. Smart Grid 2014, 5, 2635–2643.

[20]. Mehrizi-Sani, A.; Iravani, R. Potential-function based control of a microgrid in islanded and grid-connected modes. IEEE Trans. Power Syst. 2010, 25, 1883–1891.